0026-895X/98/060968-11$3.00/0

MOLECULAR PHARMACOLOGY, **54:**968–978 (1998).

A Hydrophobic Cluster between Transmembrane Helices 5 and 6 Constrains the Thyrotropin-Releasing Hormone Receptor in an Inactive Conformation

ANNY-ODILE COLSON, JEFFREY H. PERLMAN, ARTI JINSI-PARIMOO, DANIEL R. NUSSENZVEIG, ROMAN OSMAN, and MARVIN C. GERSHENGORN

Department of Physiology and Biophysics, Mount Sinai School of Medicine of the City University of New York, New York, New York 10029 (A.-O.C., R.O.), and Division of Molecular Medicine, Department of Medicine, Cornell University Medical College and The New York Hospital, New York, New York 10021 (J.H.P., A.J.-P., D.R.N., M.C.G)

Received May 8, 1998; Accepted August 26, 1998

This paper is available online at http://www.molpharm.org

ABSTRACT

We have studied the role of a highly conserved tryptophan and other aromatic residues of the thyrotropin-releasing hormone (TRH) receptor (TRH-R) that are predicted by computer modeling to form a hydrophobic cluster between transmembrane helix (TM)5 and TM6. The affinity of a mutant TRH-R, in which Trp279 was substituted by alanine (W279A TRH-R), for most tested agonists was higher than that of wild-type (WT) TRH-R, whereas its affinity for inverse agonists was diminished, suggesting that W279A TRH-R is constitutively active. We found that W279A TRH-R exhibited 3.9-fold more signaling activity than WT TRH-R in the absence of agonist. This increased basal activity was inhibited by the inverse agonist midazolam, confirming that the mutant receptor is constitutively active. Computer-simulated models of the unoccupied WT TRH-R, the TRH-occupied WT TRH-R, and various TRH-R mutants predict that a hydrophobic cluster of residues, including Trp279 (TM6), Tyr282, and Phe199 (TM5), constrains the receptor in an inactive conformation. In support of this model, we found that substitution of Phe199 by alanine or of Tyr282 by alanine or phenylalanine, but not of Tyr200 (by alanine or phenylalanine), resulted in a constitutively active receptor. We propose that a hydrophobic cluster including residues in TM5 and TM6 constrains the TRH-R in an inactive conformation via interhelical interactions. Disruption of these constraints by TRH binding or by mutation leads to changes in the relative positions of TM5 and TM6 and to the formation of an active form of TRH-R.

In general, native or WT seven-TM GPCRs do not signal in the absence of agonists. However, several native GPCRs have been found to exhibit basal or constitutive activity (Arvanitakis *et al*., 1998). For example, the native mouse TRH-R was shown to be active in the absence of agonist when assayed with a sensitive reporter gene construct in which a protein kinase C-responsive promoter/enhancer regulated transcription of a firefly luciferase gene (Jinsi-Parimoo and Gershengorn, 1997). The majority of GPCRs that have been found to be basally active are, however, receptors in which mutations occurred naturally or were constructed in the laboratory (Lefkowitz *et al*., 1993). Residues whose mutations result in constitutive activation have been found most often in the third intracellular loop and TM6 but have also been found in other GPCR domains (Arvanitakis *et al*., 1998). For example, truncation of the carboxyl-terminal tail of TRH-R results in a constitutively active receptor (Matus-Leibovitch *et al*., 1995). It has been proposed that activating mutations release the native receptor from an inactive conformation (Kjelsberg *et al*., 1992), and several groups have suggested that specific interactions among residues in the helical bundle of GPCRs are involved in constraining native receptors in inactive conformations (Robinson *et al*., 1992; Scheer *et al*., 1996; Groblewski *et al*., 1997; Lin *et al*., 1997).

Our computer simulations of the TRH-R predicted that Trp279 (TM6), a highly conserved residue in GPCRs, is part of a hydrophobic cluster composed of aromatic residues in TM5 and TM6 (Gershengorn and Osman, 1996). It has been proposed that conserved residues are critical for maintaining the common topological features of GPCRs (Baldwin, 1994) and their activities (Wess *et al*., 1993). Different effects on receptor function were found, however, when a conserved

This work was supported by National Research Service Award DK09647 (A.-O.C.), National Institutes of Health Physician Scientist Award DK02101 (J.H.P.), and National Institutes of Health Grant DK43036 (M.C.G., R.O.). A.-O.C. and J.H.P. contributed equally to this work.

ABBREVIATIONS: WT, wild-type; GPCR, G protein-coupled receptor; TRH, thyrotropin-releasing hormone; TRH-R, thyrotropin-releasing hormone receptor; TM, transmembrane helix; IP, inositol phosphate; MeTRH, [*N-t*-methylhistidine]thyrotropin-releasing hormone; 1-desaza-TRH, [desazapyro-Glu]thyrotropin-releasing hormone [Na-[(1*R*)-3-oxocyclopentanecarbonyl]-L-histidyl-L-prolineamide]; bp, base pair(s); PBS, phosphate-buffered saline.

residue was mutated in different receptors (Baldwin, 1994; Van Rhee and Jacobson, 1996). In this work, we study the roles of the highly conserved tryptophan in TM6 and of other aromatic residues that form the hydrophobic cluster between TM5 and TM6 of the TRH-R. We present experimental evidence that Trp279 and Tyr282 in TM6 and Phe199 in TM5 constrain the TRH-R in an inactive conformation, confirming the predictions of our computer-generated model.

Materials and Methods

Computer modeling. We previously constructed models of the TRH/WT TRH-R complex using mixed-mode Monte Carlo/stochastic dynamics simulations, which led to the definition of a transmembrane binding pocket (Laakkonen *et al*., 1996). Simulation of the binding pocket is in good agreement with experimental findings (Gershengorn and Osman, 1996). The extracellular loops of the receptor were subsequently constructed (Colson *et al*., 1998). The intracellular loops in the WT TRH-R, with and without bound TRH, were constructed using the protocol described in our previous work.

To examine the effects of mutation of Trp279, Phe199, Tyr200, and Tyr 282 on receptor structure and dynamics, we constructed several models of the mutant receptors by substituting alanine for Trp279, Phe199, Tyr200, and Tyr282 and phenylalanine for Tyr200, at the end of a 100-psec simulation of the unoccupied receptor. The system was energy-minimized and heated to 300°K in 23 psec, and molecular dynamics simulations were performed at 300°K for 1 nsec. A 1-nsec simulation was also performed for the unoccupied and occupied WT TRH-Rs.

In all calculations, a distance-dependent dielectric function was used to approximate the effects of the environment. All calculations were performed with the CHARMM program, ver. 23 (Brooks *et al*., 1983).

Materials. [^{3}H]MeTRH was obtained from DuPont New England Nuclear. *myo*-[^{3}H]Inositol was from Amersham. TRH was from Calbiochem and MeTRH from Sigma. Dulbecco's modified Eagle's medium and fetal calf serum were from Collaborative Research. 1-Desaza-TRH and 2-iodo-TRH were generous gifts from L. A. Cohen (National Institutes of Health). Pyr3-TRH and ProMe3-TRH were generous gifts from T. K. Sawyer (Parke-Davis Pharmaceutical Research) and C. Y. Bowers (Tulane Medical Center), respectively. Val2-TRH was from Peninsula. Plasmid containing a protein kinase C-responsive promoter element fused to the firefly luciferase gene (AP1-*fos*-Luc) was a generous gift from P. J. Deutsch (previously of Cornell University Medical College) (Schadlow *et al*., 1992). All other reagents were from Sigma.

DNA. Plasmid pCDM8 containing an insert encoding WT mouse TRH-R (pCDM8mTRHR), as described previously (Perlman *et al*., 1995), was used for transfection. Plasmid pCDM8 containing an insert encoding W279A TRH-R was constructed as previously described (Perlman *et al*., 1995). The polymerase chain reaction was used to generate fragments containing the Y200A and F199A mutations, the fragments were subcloned into plasmid Bluescript encoding WT TRH-R, and a fragment derived from digestion with *Xho*I and *Not*I was then subcloned into pCDM8mTRHR. Mutations were confirmed by sequencing using the dideoxy chain termination method.

To construct FLAG epitope-tagged receptors, we synthesized a cDNA encoding a chimeric protein in which the initiating methionine of TRH-R was replaced with the amino acid sequence of the prolactin leader, followed by the FLAG epitope and then the amino-terminal ectodomain of the human calcitonin receptor (Nussenzveig *et al*., 1994). Three DNA fragments, which were obtained as follows, were ligated together. 1) A mammalian expression plasmid (pMT4) encoding the TRH-R (Nussenzveig *et al*., 1994) was digested with *Eco*RI and *Xho*I, and the resulting 6272-bp DNA was purified by agarose gel electrophoresis and Geneclean procedure (Bio 101). 2) A 795-bp DNA fragment was generated by polymerase chain reaction using plasmid Bluescript encoding WT TRH-R as template and sense (5′-GCGAATGCATACGAGAATGATACTGTCAGTG-3′) and antisense (5′-CTTCCTGGAGCTCACAGTGCTGTTGAAGCATC-3′) primers; the fragment was purified with Geneclean. The fragment was digested with *Nsi*I and *Xho*I, and the resulting 65-bp fragment was purified by agarose gel electrophoresis and the Mermaid procedure (Bio 101). 3) A DNA fragment encoding the prolactin leader-FLAG-human calcitonin receptor amino terminus was generated by *Eco*RI/*Nsi*I digestion of a plasmid encoding a FLAG epitope-tagged human calcitonin receptor (Cohen *et al*., 1997) to yield a 488-bp fragment, which was purified by agarose gel electrophoresis and Geneclean. This yielded a plasmid (pMT4-FLAG-WT TRH-R) encoding a chimeric receptor (FLAG-WT TRH-R) with a prolactin signal sequence followed by the FLAG epitope (DYKDDDDK), residues from Leu23 to Tyr146 of the human calcitonin receptor, and residues from Glu2 to the end of the mouse TRH-R. The amino terminus of the calcitonin receptor was added to the chimeric receptor to permit recognition by the anti-FLAG M2 monoclonal antibody; a receptor with a FLAG epitope added in place of the initiating methionine of mouse TRH-R was not recognized by the M2 antibody when expressed in COS-1 cells (data not shown). FLAG-WT TRH-R binds [^{3}H]MeTRH and signals in response to TRH in a manner indistinguishable from that of WT TRH-R (data not shown). FLAG epitope-tagged mutant TRH-Rs were constructed by inserting the fragment from the *Xho*I/*Not*I digestion of pCDM8 encoding the mutant TRH-R into *Xho*I/*Not*Idigested pMT4FLAG-WT TRH-R.

Cell culture and transfection. COS-1 cells were maintained and transiently transfected, using the DEAE-dextran method, as previously described (Perlman *et al*., 1995). In brief, cells were seeded 1 or 2 days before transfection, at 0.7–1.5 $\times$ 10^6 cells/100-mm dish. After transfection, cells were maintained in Dulbecco's modified Eagle's medium with 10% fetal calf serum for 1 day; cells were then harvested and seeded into 12-well plates, at 100,000 cells/well, in Dulbecco's modified Eagle's medium with 5% fetal calf serum. AtT-20 cells were maintained and stably transfected as described (Perlman *et al*., 1995).

Receptor binding studies. One day after reseeding into 12-well plates, competition binding experiments were carried out for 4 hr at 4° with cells in monolayer, in buffer with 2 nM [^{3}H]MeTRH and unlabeled analogs as described (Colson *et al*., 1998). K_i values were derived from competition binding experiment data, for which curves were fitted by nonlinear regression analysis and drawn with the PRISM program (GraphPad Inc.).

Anti-FLAG M2 chemiluminescence assay in COS-1 cells. Cells were transfected as described above and seeded (up to 40,000 cells/well) in 96-well plates. On day 2, cells were washed twice with PBS (1$\times$ = 100 mM NaCl, 55 mM sodium phosphate, pH 7.3) containing 2 mM levels of Ca^{2+} and Mg^{2+} and were incubated for 1 hr at room temperature with a "blocking solution" [10% (w/v) dry milk in PBS]. Cells were washed twice and incubated for 1 hr at room temperature with anti-FLAG M2 antibody (1/300 dilution in PBS with 0.5% bovine serum albumin and 0.1% sodium azide; Eastman Kodak Co.); cells were then washed twice and incubated for 1 hr at room temperature with secondary β-galactosidase-conjugated antibody (1/5000 dilution in PBS with 0.5% bovine serum albumin and 0.1% sodium azide). After incubation, the cells were washed twice, 100 μl of Galacton-Star/Sapphire-II substrate/enhancer formulation (TROPIX) was added to each well, cells were incubated for 40 min, and the luminescence was measured for 10 sec.

Luciferase activity assay. Cells were co-transfected with plasmid encoding TRH-R (2 μg/ml, unless otherwise indicated) and 2–5 μg/ml plasmid containing AP1-*fos*-Luc and were incubated in Dulbecco's modified Eagle's medium containing 10% serum. TRH stimulation of luciferase gene transcription was measured by adding 10 μM TRH to cells for the last 4 hr of incubation (between 44 and 48 hr). Where indicated, midazolam was added immediately after transfec-

tion. Luciferase activity was assayed as described (Jinsi-Parimoo and Gershengorn, 1997), at 48 hr.

Results and Discussion

To characterize the role of Trp279 in TM6 of TRH-R, Trp279 was replaced by alanine (yielding W279A TRH-R). Competition binding between [^{3}H]MeTRH and a series of unlabeled TRH analogs (all agonists) was measured for WT and W279A TRH-Rs expressed in COS-1 cells (Table 1). The affinity of WT TRH-R for MeTRH was 6-fold higher than that for TRH, and the affinities for 1-desaza-TRH, Val2-TRH, 2-iodo-TRH, Pyr3-TRH, and ProMe3-TRH were 320-, 1200-, 92-, 840-, and 49-fold lower, respectively, than that for TRH. The affinities of W279A TRH-R for MeTRH and 2-iodo-TRH were similar to those of the WT TRH-R; the affinities for TRH, 1-desaza-TRH, Val2-TRH, Pyr3-TRH, and ProMe3-TRH were 6-, 34-, 24-, 7-, and 16-fold higher, respectively, than those of the WT TRH-R. Thus, for five of seven agonists tested, but not for MeTRH or 2-iodo-TRH, the affinities of W279A TRH-R were higher than those of WT TRH-R. These observations are consistent with the idea that W279A TRH-R is more constitutively active than WT TRH-R (see below).

A current model of GPCR activation is the allosteric ternary complex model, which includes an equilibrium between two states of the unoccupied receptor, namely an inactive state (R) and an active receptor state (R*) (Samama *et al.*, 1993). The model proposes that agonists prefer to bind R* and inverse agonists (i.e., agents that inhibit basal activity, also referred to as negative antagonists) prefer to bind R. It follows from this prediction that constitutively active mutant GPCRs would bind agonists with higher affinity than WT receptors and would bind inverse agonists with lower affinity than WT receptors (Lefkowitz *et al.*, 1993). This prediction has been confirmed for many, but not all, GPCR/ligand systems (Tiberi and Caron, 1994; Spalding *et al.*, 1995). The higher affinity of W279A TRH-R for most agonists tested was consistent with the idea that W279A TRH-R is constitutively active. To further characterize the binding profile of W279A TRH-R, binding of competitive inverse agonists was measured. The affinities of W279A TRH-R for midazolam and chlordiazepoxide, two benzodiazepine drugs that are competitive inverse agonists at the TRH-R (Jinsi-Parimoo and Gershengorn, 1997) (see below), were 3.4-and 6.5-fold lower, respectively, than those of WT TRH-R. These data are also consistent with the idea that W279A TRH-R is more constitutively active than WT TRH-R.

We previously expressed W279A TRH-Rs in COS-1 cells and measured IP second messenger formation (Perlman *et al.*, 1995). TRH stimulated IP formation to the same maximal extent in cells expressing W279A TRH-Rs and cells expressing WT TRH-Rs (see below), but there was no detectable TRH-independent formation of IPs in COS-1 cells expressing WT or W279A TRH-Rs. We also stably expressed WT and W279A TRH-Rs in mouse pituitary AtT-20 cells. As with COS-1 cells expressing WT or W279A TRH-Rs, no stimulation of IP formation was observed in AtT-20 cells expressing these receptors, in the absence of a TRH agonist (data not shown).

By using an assay system more sensitive than IP formation, we showed previously that WT TRH-R is basally active (Jinsi-Parimoo and Gershengorn, 1997). A plasmid construct

TABLE 1
Binding affinities of WT and W279A TRH-Rs for agonists and antagonists
Binding experiments were conducted at 4° with cell monolayers in duplicate, as described in Materials and Methods. The number of experiments is given in parentheses. Variance is given as the standard error for more than two experiments and as the range for two experiments.

TRH-R	K_i									
	Agonists							Antagonists		
	TRH	MeTRH	1-Desaza-TRH	Val2-TRH	2-Iodo-TRH	Pyr3-TRH	ProMe3-TRH	Midazolam	Chlordiazepoxide
	nM									
WT	37 ± 11 (6)	6.1 ± 0.8 (14)	12,000 (4,700–19,000) (2)	44,000 ± 8,500 (3)	3,400 ± 620 (4)	31,000 (18,000–44,000) (2)	1,800 (1,800–1,800) (2)	50 ± 9.0 (6)	130 ± 11 (8)
W279A	6.2 ± 1.5 (4)	6.5 ± 0.7 (7)	350 (320–380) (2)	1,800 (1,400–2,100) (2)	2,400 (1,900–2,900) (2)	4,300 (4,100–4,400) (2)	110 (55–160) (2)	170 ± 8.8 (3)	840 ± 170 (5)

in which a protein kinase C-responsive promoter/enhancer regulates transcription of a firefly luciferase gene (AP1-*fos*-Luc) was coexpressed in COS-1 cells with WT or W279A TRH-Rs. For WT or W279A TRH-Rs, a maximal level of luciferase activity was reached after 48 hr. At all time points at which luciferase activity was detectable, the level was higher in cells expressing W279A TRH-Rs than in those expressing WT TRH-Rs (data not shown). The effect of increases in the number of expressed receptors (produced by varying the amount of plasmid in the transfection cocktail) on luciferase activity in the absence of agonist was determined (Fig. 1). The slope of the relationship between receptor level and basal activity for WT TRH-R was significantly greater than zero, confirming that the WT TRH-R is constitutively active. Importantly, the slope of the line describing the relationship between receptor expression and basal activity for W279A TRH-R was 3.9 ± 1.0-fold greater than that for WT TRH-R (nine experiments, $p < 0.007$, paired one-tailed t test). Therefore, W279A TRH-R is significantly more constitutively active than is WT TRH-R.

The specificity of the basal signaling activity was indicated by the direct relationship between TRH-R expression and luciferase activity shown in Fig. 1. To confirm this specificity, incubations in the presence of the competitive inverse agonist midazolam were performed. Benzodiazepines do not affect luciferase activity in cells expressing luciferase without TRH-Rs, and they do not affect TRH-R number under these conditions (Jinsi-Parimoo and Gershengorn, 1997). Basal luciferase activity was completely inhibited by 100 μM midazolam in cells expressing either WT or W279A TRH-Rs (data not shown). This confirms our previous finding that midazolam is an inverse agonist of WT TRH-R (Jinsi-Parimoo and Gershengorn, 1997). The IC_{50} for this effect was 2.1-fold higher for W279A TRH-R (26 ± 4.5 μM) than for WT TRH-R (13 ± 3.5 μM), consistent with the observed difference in binding affinity.

Mixed-mode Monte Carlo/stochastic dynamics simulations performed previously in our laboratory (Laakkonen *et al.*, 1996) showed that Trp279 is part of a hydrophobic cluster in the transmembrane bundle of the WT TRH-R. To further examine the behavior of this highly conserved residue, we

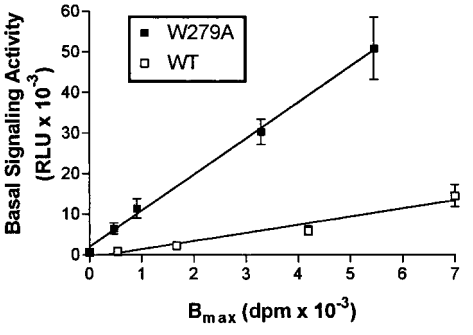

Fig. 1. Basal luciferase activity as a function of the number of WT or W279A TRH-Rs expressed on the cell surface. COS-1 cells were cotransfected with plasmid containing AP1-*fos*-Luc and various amounts of plasmid encoding TRH-R (0.7, 2, 7, or 20 ng/ml in this representative of nine experiments) and were assayed for luciferase activity as described in Materials and Methods. Results are expressed as mean ± standard deviations of assays performed in triplicate. In this experiment, the slopes of the relationships between B_{max} and basal activity were 7.5 (5.2–9.8) × 10^{-4} and 29 (23–35) × 10^{-4} for WT and W279A TRH-Rs, respectively. Receptor expression was determined by 2 nM [^{3}H]MeTRH binding, in monolayers, at 37° for 1 hr. *RLU*, relative light units.

conducted long (1-nsec) molecular dynamics simulations of WT TRH-R with and without bound TRH. In the unoccupied WT receptor, the χ_1 torsional angle (C-Cα-Cβ-Cγ) of Trp279 calculated from the molecular dynamics trajectory is, on average, 80 ± 11°. This indicates that the ring of Trp279 is parallel to the membrane and is involved in stacking interactions with its neighboring residues, which constrain this region of the receptor (Fig. 2). In the TRH-occupied WT receptor, however, the χ_1 angle of Trp279 is 152 ± 11°, which results in the plane of the ring being nearly perpendicular to the membrane, as shown in an energy-minimized structure obtained over the last 200 psec of the trajectory presented in Fig. 2. Such a conformational change of Trp279 induced by the binding of TRH in the transmembrane binding pocket contributes to the release of constraints generated by the stacking interactions that were present in the unoccupied WT receptor.

To gain insight into the mechanism by which constitutive activity arises, we performed and analyzed a 1-nsec molecular dynamics simulation of W279A TRH-R. Comparison of energy-minimized average structures of W279A and WT TRH-Rs shows significant variations in the distance between the segments of TM5 and TM6 that are connected to the putative third intracellular loop (i.e., the distance between the Cα atoms of Phe213 and Gln263). This observation led us to analyze the 1-nsec trajectories of the unoccupied WT, TRH-occupied WT, and W279A TRH-Rs (2000 structures in each trajectory) to obtain a distribution of distances between the residues directly attached to intracellular loop 3 in TM5 and TM6. The results presented in Fig. 3 indicate unimodal distance distributions for unoccupied and TRH-occupied WT TRH-Rs. This representation also shows that the average distance between the intracellular portions of TM5 and TM6 in the unoccupied WT TRH-R is approximately 3.0 Å shorter than that in the TRH-occupied WT receptor. If the increased distance between TM5 and TM6 in the TRH-occupied WT receptor reflects a change that leads to constitutive activity, it is expected that similar changes in the relative positions of TM5 and TM6 would be observed in the mutant W279A receptor. A similar analysis performed on W279A TRH-R revealed that the distribution of distances between the intracellular portions of TM5 and TM6 is bimodal. The peak centered around 15.3 Å represents distances in 65% of the structures in the stable portion of the trajectory (see below). This distribution is comparable to that observed in the TRH-occupied WT receptor (Fig. 3A). Thus, these data are consistent with the idea that an increased distance between residues at the intracellular borders of TM5 and TM6 is associated with an activated signaling state of the TRH-R.

It has been suggested that reorganization of rhodopsin during the R→R* conformational transition increases the polarity of the environment of tryptophan residues (Lin and Sakmar, 1996). If such a mechanism also occurs in the TRH-R, it would be consistent with disruption of the closely packed hydrophobic cluster of aromatic residues around Trp279. The hydrophobic cluster surrounding Trp279 is composed of Phe196, Phe199, Tyr200, Phe275, and Tyr282. Because disruption of this hydrophobic pocket upon mutation of Trp279 to alanine results in a constitutively active receptor, we hypothesized that mutation of other residues that are part of the hydrophobic cluster could also result in constitutive activity. Among these residues, the side chains of Phe199

and Tyr282 are directed into the core of the transmembrane bundle, whereas that of Tyr200 is directed to the outside of the bundle (Fig. 4) and interacts only loosely with other residues of the hydrophobic pocket. We therefore predicted that the hydrophobic cluster would be significantly disrupted upon mutation of Phe199 or Tyr282, leading to a constitutively active receptor, whereas mutation of Tyr200 would have little or no effect on the overall conformation of the cluster and should not lead to constitutive activity. Distance distributions between residues proximal to intracellular loop 3 in TM5 and TM6 (i.e., the Cα atoms of Phe213 and Gln263) were obtained from the 1-nsec molecular dynamics simulations of F199A, Y200A, and Y200F TRH-Rs. The results presented in Fig. 3B show that the unimodal distribution obtained with F199A TRH-R is similar to that obtained with W279A TRH-R (Fig. 3A), with an average distance between Phe213 and Gln263 of 14.3 Å, whereas distances in Y200A, Y200F (not shown), and empty WT TRH-Rs were distributed around 11.5, 11.1, and 12.0 Å, respectively (Fig. 3B). In addition, it is interesting to compare the time of evolution of this distance in W279A, F199A, and WT TRH-Rs during the simulations (Fig. 3B, *inset*). The maximal distance between the intracellular portions of TM5 and TM6 is reached nearly 200 psec earlier in F199A TRH-R, compared with W279A TRH-R. These findings confirm that in our model F199, but not Y200, is important in constraining TM5 and TM6, and they lead to the predictions that F199A TRH-R would be more and Y200A TRH-R would be less constitutively active than W279A TRH-R.

To test these predictions, we constructed and characterized F199A and Y200A TRH-Rs. There was no high affinity binding of [^{3}H]MeTRH to F199A and Y200A TRH-Rs. It is likely that the markedly lowered affinity of these two receptor mutants is the result of the effects of these mutations on the TRH binding pocket (Gershengorn and Osman, 1996). These findings demonstrate a problem in the interpretation of findings with mutated receptors, namely that even site-specific substitutions often affect more than one receptor function (in

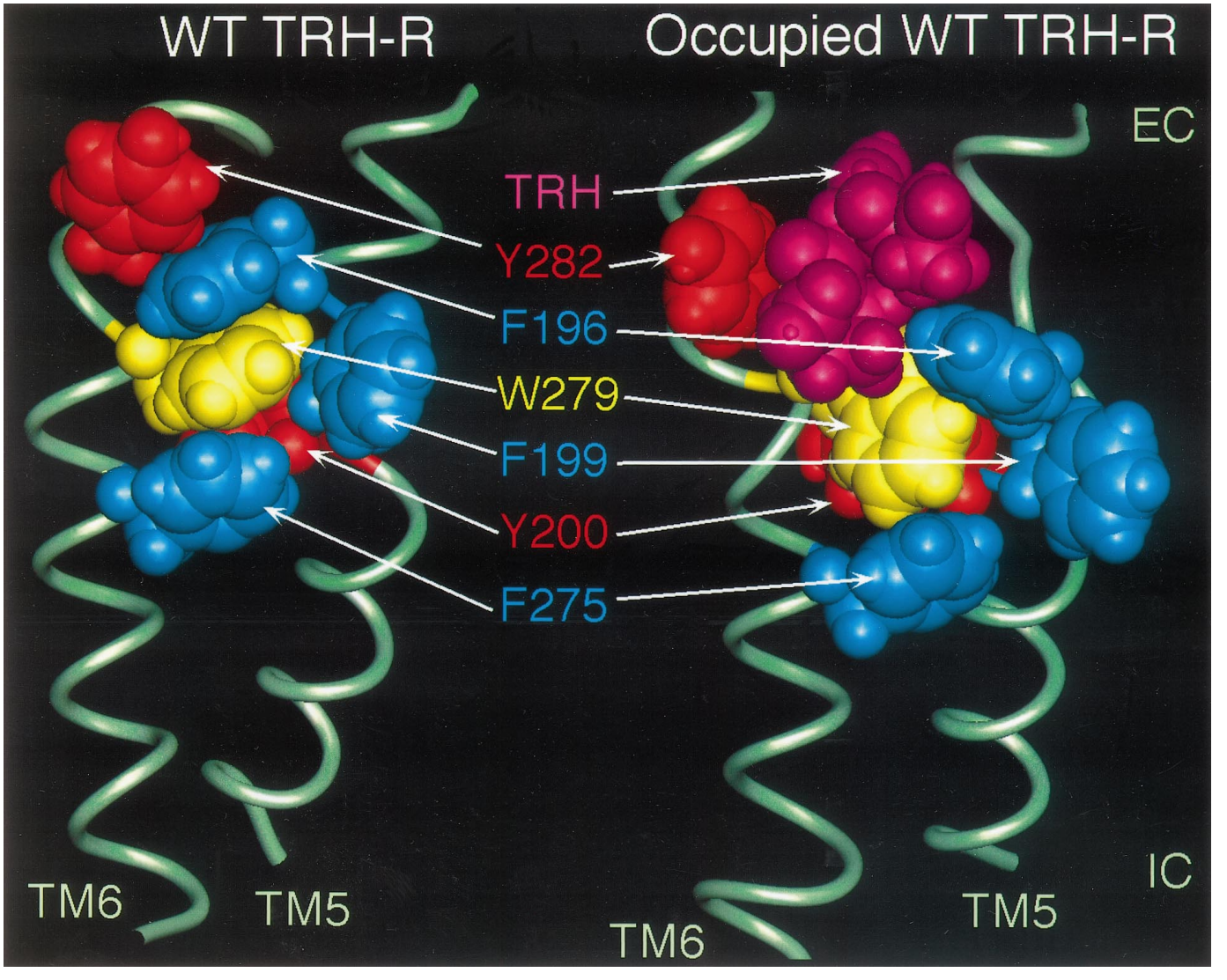

Fig. 2. Model of the hydrophobic cluster formed by aromatic residues in TM5 and TM6 of the WT and TRH-occupied WT TRH-Rs. The structures presented were extracted from averaged minimized structures derived from the last 200 psec of 1-nsec simulations, as described in Materials and Methods. The receptor is positioned so that its extracellular domain is at the *top*. The core of the receptor is in the foreground. For clarity, only TM5 and TM6 are displayed. The hydrophobic cluster is composed of the following residues: Phe196 (*F196*), Phe199 (*F199*), and Tyr200 (*Y200*) in TM5 and Phe275 (*F275*), Trp279 (*W279*), and Tyr282 (*Y282*) in TM6.

this instance, binding of ligand and basal signaling activity; see below). To measure the expression of receptors that do not bind [^{3}H]MeTRH with high affinity, we constructed TRH-Rs containing the FLAG epitope in their amino termini. Fig. 5 illustrates that FLAG epitope-tagged and untagged TRH-Rs are stimulated by TRH to produce IPs to the same maximal extents. Using an antibody-based chemiluminescence assay, we found that WT, W279A, F199A, and Y200A

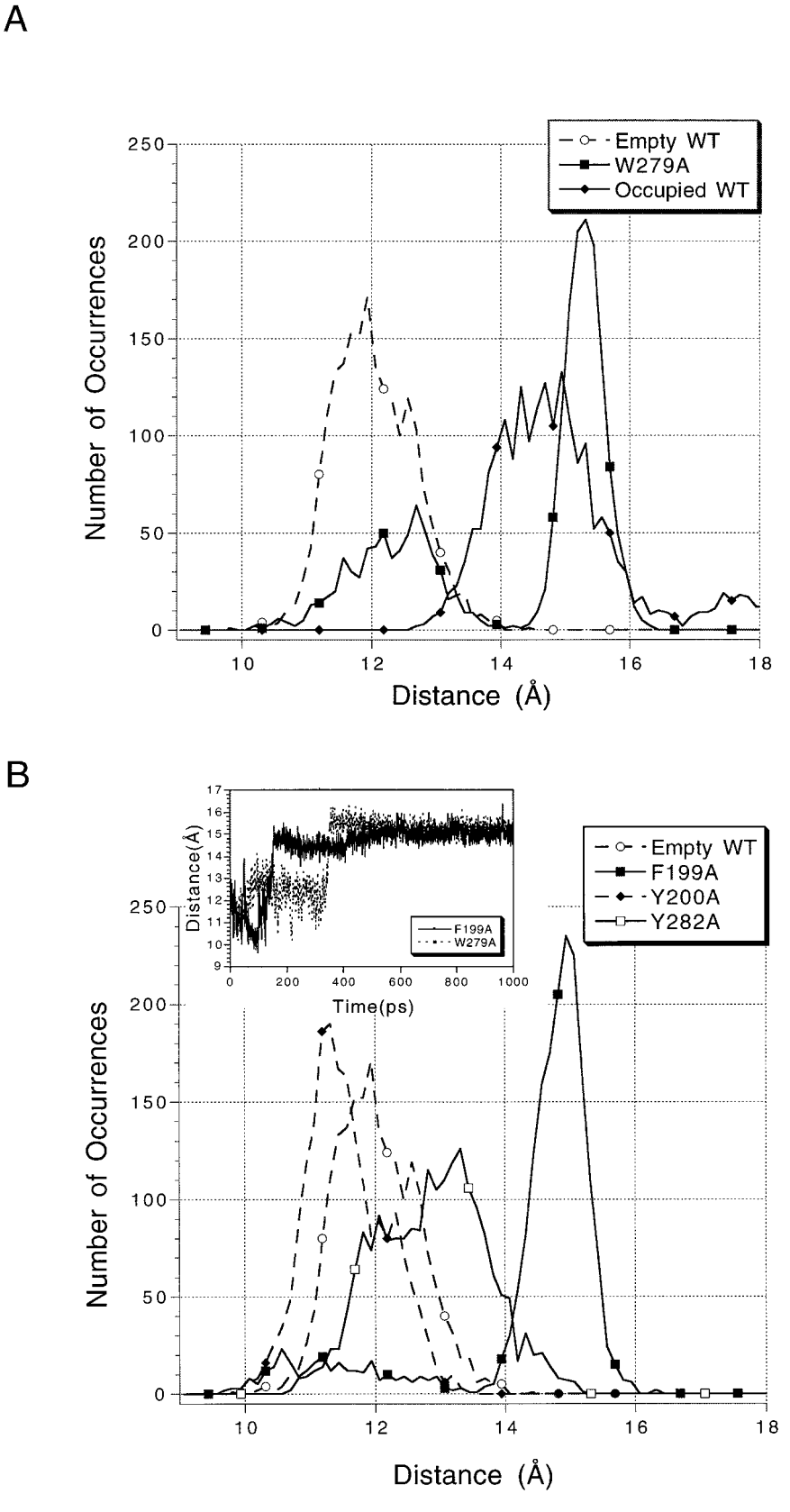

Fig. 3. Distribution of distances between the Cα atom of Phe213 in TM5 and Gln263 in TM6 throughout 1-nsec (i.e., 2000 structures) computer-simulated trajectories of the empty WT, W279A, and TRH-occupied WT TRH-Rs (A) and empty WT, F199A, Y200A, and Y282A TRH-Rs (B). *Inset*, evolution of this distance in the F199A and W279A TRH-Rs throughout the 1-nsec trajectories.

TRH-Rs were expressed to similar levels in COS-1 cells (Fig. 6). We were, therefore, able to compare the intrinsic basal signaling activities of these TRH-Rs under our standard conditions. Using the luciferase assay (see above), we found that F199A TRH-R exhibited a higher basal signaling activity than did W279A TRH-R, whereas Y200A TRH-R was only as active as WT TRH-R (Figs. 6 and 7B). As with W279A TRH-R, there was no effect on basal IP formation in COS-1 cells expressing either of these receptor mutants, but TRH caused dose-dependent stimulation of IP formation in cells expressing F199A and Y200A TRH-Rs. As predicted from the lack of high affinity binding, the potencies for TRH-stimulated signaling by F199A and Y200A TRH-Rs were decreased, compared with WT and W279A TRH-Rs; the EC_{50} values were 210 nM (95% confidence interval, 110–390 nM) for F199A TRH-R and 7.2 nM (2.4–22 nM) for Y200A TRH-R (data not shown), compared with 1.1 nM for WT and W279A TRH-Rs (Perlman *et al.*, 1995). For all four TRH-Rs tested, the maximal levels of TRH stimulation of IP formation varied directly with the amount of plasmid included in the transfection cocktail (Fig. 7A), consistent with the idea that more receptors were expressed in transfections with larger amounts of plasmid. These data are consistent with our model.

Our model suggests that another hydrophobic residue, Tyr282, which is positioned above W279, is also part of the cluster and is directed into the core of the transmembrane bundle (Fig. 4). Tyr282 is hydrogen-bonded to Tyr192 in the unoccupied receptor and is in close proximity to W279. In the occupied receptor, the hydrogen bond to Tyr192 is replaced by an interaction with the backbone of TRH, and the aromatic ring of Tyr282 stacks on the histidine side chain of TRH. It appears that Tyr282 constrains the unoccupied receptor in its inactive form. It is therefore anticipated that mutation of Y282 should relieve the constraint and generate a constitutively active receptor. A 1-nsec simulation of the Y282A TRH-R mutant shows a bimodal distribution of the distances between the intracellular portions of TM5 and TM6 (Fig. 3B). The peak centered around 13.2 Å represents distances calculated in 70% of the structures. It corresponds to a distance located halfway between the distances calculated in the unoccupied receptor and the F199A and W279A receptors, which suggests that constitutive activity should be observed with the mutant receptor.

To further test the predictions of our model, we studied the basal signaling activities of Y282A and Y282F TRH-Rs. Y282A and Y282F TRH-Rs exhibited basal signaling activities that were higher than that of WT TRH-R (1.7 ± 0.26- and 1.9 ± 0.25-fold higher than that of WT TRH-R, respectively) (Fig. 8) but were not as high as those of W279A or F199A TRH-Rs. We also investigated whether there was any effect of the substitution of these hydrophobic residues on TRH induction of gene transcription (Fig. 8). The absolute levels of maximal induction by TRH were similar in cells expressing all of these mutant TRH-Rs. When the induction produced by TRH was analyzed as fold increases above basal activity, then the cells expressing F199A and W279A TRH-Rs, which are the most basally active receptors, exhibited lowered fold induction, compared with cells expressing the other TRH-Rs. This may be because the cells cannot increase transcription of the luciferase gene above this apparent maximal level or because the more basally active receptors cause the cells to be desensitized to TRH. The former seems more likely, because levels of TRH-stimulated signaling by F199A and W279A TRH-Rs, measured as IP formation, were similar in cells expressing all of these TRH-Rs (Figs. 5 and 7) (Perlman *et al.*, 1996). Therefore, our model correctly predicted which of four mutations of proximate aromatic amino acid residues in a hydrophobic pocket of TRH-R would lead to constitutive activity and which would not.

Our computer-generated model predicts that significant movement occurs in the region in TM5 proximal to the third intracellular loop (see above) but that much less motion is observed at the extracellular end of the helix (Fig. 9). This suggests that the hydrophobic cluster described above constrains WT TRH-R primarily at the extracellular side of the TM. Disruption of this hydrophobic pocket by mutation of residues within the cluster, or by binding of TRH (Fig. 1),

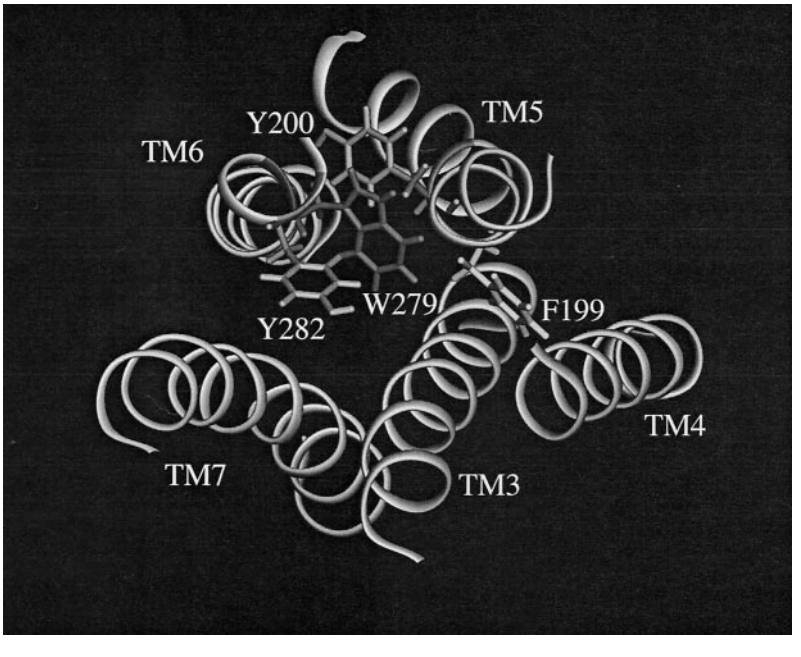

Fig. 4. Model showing the positions of Phe199 (*F199*), Tyr200 (*Y200*), Trp279 (*W279*), and Tyr282 (*Y282*) in the unoccupied WT TRH-R. Y200 is directed to the outside of the transmembrane bundle, and F199 and Y282 are directed into the core of the transmembrane bundle. The structure presented was extracted from averaged minimized structures derived from the last 200 psec of a 1-nsec simulation. The receptor is positioned so that its extracellular domain is in the foreground. For clarity, TM1 and TM2 have been omitted.

results in receptor activation. A similar observation regarding constraint of helices 5 and 6 by a hydrophobic cluster of residues has been made in studies of the lutropin/choriogonadotropin receptor (Lin *et al*., 1997). In that case, the cluster appears to be within the intracellular part of the helices, rather than nearer the extracellular region, as in TRH-R. However, the exact boundaries of the helices in GPCRs are not known and the hydrophobic cluster may be comparable in the two receptors. Nevertheless, it appears that different GPCRs use interactions between hydrophobic residues in helices 5 and 6 to constrain the receptor in an inactive state. Loss of a constraint present in native GPCRs has been proposed as a general mechanism of GPCR activation (Lefkowitz *et al*., 1993). A result of loss of a constraint may be increased mobility of domains within the receptor protein, and several reports have presented evidence that increased intramolecular mobility is associated with GPCR activation. For example, studies with spin-labeled rhodopsin are consistent with the idea that TM5 and the intracellular loop that connects it to TM6 are more mobile upon photoactivation (Altenbach *et al*., 1996; Farrens *et al*., 1996), and studies of a fluorescently labeled, constitutively active, α_{1B}-adrenergic receptor are consistent with it exhibiting increased mobility, compared with the WT receptor (Gether *et al*., 1997; Javitch *et al*., 1998). Because a tryptophan in TM6 corresponding to Trp279 in TRH-R is conserved among the rhodopsin/β-adrenergic receptor subfamily of GPCRs (Probst *et al*., 1992), it is important to determine whether this tryptophan plays a general role in maintaining the inactive state. However, replacement of the conserved tryptophan by phenylalanine did not result in a basally active m3 muscarinic receptor, possibly because phenylalanine may form an aromatic interaction like tryptophan and thereby effectively maintain an inactive

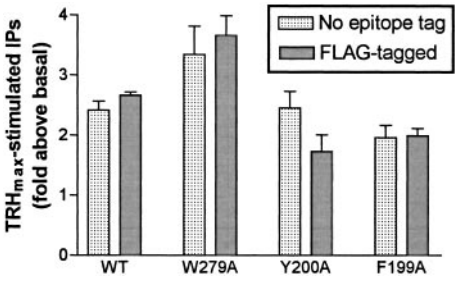

Fig. 5. TRH stimulation of IP second messenger formation in FLAG epitope-tagged and untagged TRH-Rs. COS-1 cells were transfected with plasmid encoding TRH-Rs (2000 ng/ml) and were assayed for TRH stimulation of IP formation as described in Materials and Methods. Results are expressed as mean ± standard deviation of assays performed in triplicate in a representative of three experiments.

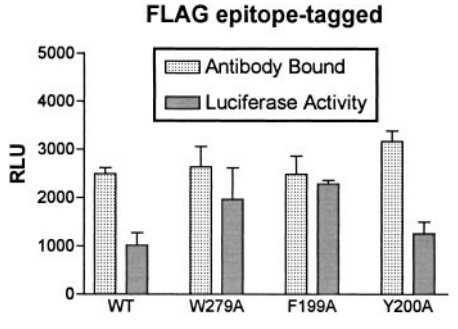

Fig. 6. Expression levels and basal signaling activities of WT, W279A, F199A, and Y200A TRH-Rs. COS-1 cells were co-transfected with plasmid containing AP1-*fos*-Luc and plasmid encoding TRH-Rs (100 ng/ml) and were tested for receptor expression by antibody-based chemiluminescence assays or basal signaling activity assays, as described in Materials and Methods. Results are expressed as mean ± standard deviation of assays performed in duplicate in two experiments. *RLU*, relative light units.

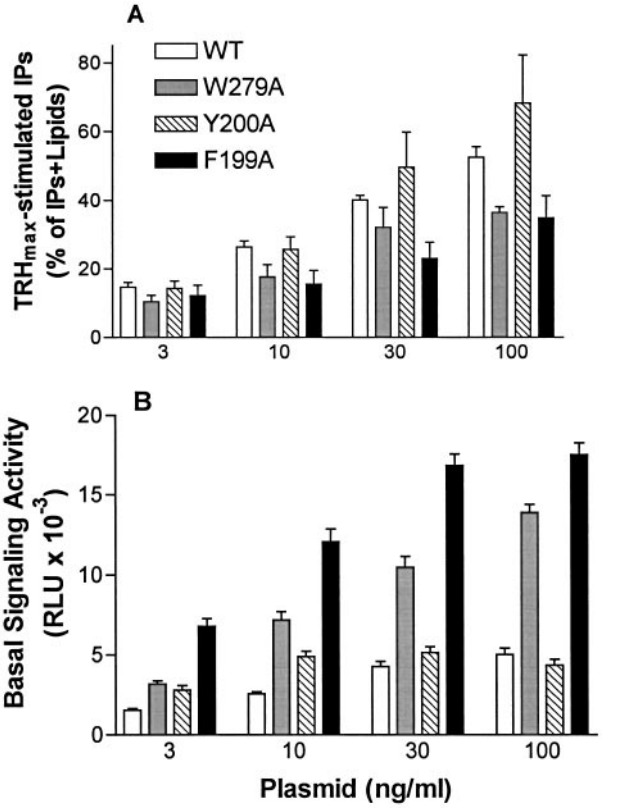

Fig. 7. TRH-stimulated IP second messenger formation and basal signaling activities as a function of the amount of plasmid encoding WT, W279A, F199A, or Y200A TRH-Rs used for transfection. COS-1 cells were co-transfected with plasmid containing AP1-*fos*-Luc and with various amounts of plasmid encoding TRH-Rs (3, 10, 30, or 100 ng/ml) and were assayed for TRH stimulation of IP formation (A) or basal signaling activities (B), as described in Materials and Methods. Results are expressed as mean ± standard deviation of assays performed in triplicate in three experiments. *RLU*, relative light units.

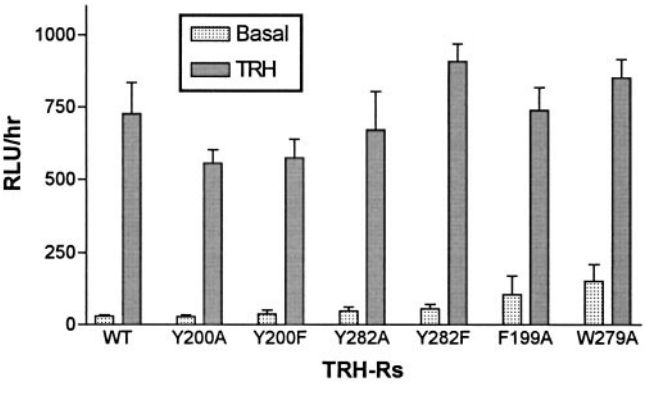

Fig. 8. Basal and TRH-stimulated signaling activities of WT, Y200A, Y200F, Y282A, Y282F, F199A, and W279A TRH-Rs. COS-1 cells were co-transfected with plasmid containing AP1-*fos*-Luc and plasmid encoding TRH-Rs (100 ng/ml), and basal and TRH-stimulated (10 μM TRH for 4 hr) signaling activities were measured, as described in Materials and Methods. Results are expressed as mean ± standard deviation of assays performed in triplicate or quadruplicate in two experiments. *RLU*, relative light units.

state (Wess *et al.*, 1993). Replacement of tryptophan by alanine in the AT_{1A} angiotensin receptor resulted in lowered agonist affinity and no change in affinity for antagonists, changes that are not suggestive of constitutive activity, but basal activity was not directly measured (Yamano *et al.*, 1995). Thus, a role for this conserved tryptophan in constraining other GPCRs in an inactive state has not been shown.

The tryptophan in TM6 has been shown to be important in other aspects of GPCR structure and function. In the m3 muscarinic receptor, its replacement by phenylalanine led to decreased maximal activity of approximately 70% of WT receptor activity (Wess *et al.*, 1993). In the AT_{1A} angiotensin receptor, it has been proposed that this tryptophan is involved in ligand binding, because it may stabilize an ionic bridge between a lysine in TM5 (adjacent to the position homologous to that of Phe196 in TM5 of TRH-R) and the terminal carboxylate of angiotensin II (Yamano *et al.*, 1995). In rhodopsin, the tryptophan in TM6 was shown to interact strongly with retinal, and it was proposed to be critical for activation (Nakayama and Khorana, 1991; Lin and Sakmar, 1996). Thus, although the tryptophan in TM6 is important, its predominant role, as determined thus far, appears to differ among members of the rhodopsin/β-adrenergic receptor subfamily of GPCRs. It may be that this tryptophan is conserved for a common critical reason that has not yet been determined or that its role has changed in different GPCRs during evolution.

Other conserved residues have been proposed to be critical for maintaining the inactive state of GPCRs. In the α-factor receptor, which does not contain the conserved tryptophan in TM6, mutation of a nearby conserved proline resulted in constitutive activity (Konopka *et al.*, 1996). The negative charge of an aspartate in TM2 of the bradykinin receptor was found to be necessary to prevent basal activation (Quitterer *et al.*, 1996). An arginine of the Glu(Asp)-Arg-Tyr sequence at the bottom of TM3 in the α_{1B}-adrenergic receptor has been proposed to interact with a highly conserved transmembrane polar pocket, consisting of an asparagine in TM1, an aspartate in TM2, an asparagine in TM7, and a tyrosine in TM7, to constrain the receptor in an inactive conformation (Scheer *et al.*, 1996). Evidence for interactions among an asparagine in TM1, an aspartate in TM2, and an asparagine in TM7 in TRH-R has also been presented (Perlman *et al.*, 1997). It is noteworthy, however, that mutation of the same conserved residue in the α_{1B}-adrenergic receptor and TRH-R causes different effects. For example, replacement of asparagine in TM1 by alanine in the α_{1B}-adrenergic receptor leads to a GPCR that is basally active and can be activated by agonist to the same level as the WT receptor (Scheer *et al.*, 1996), whereas the mutant TRH-R with substitution of asparagine in TM1 by alanine exhibits no increase in basal activity and

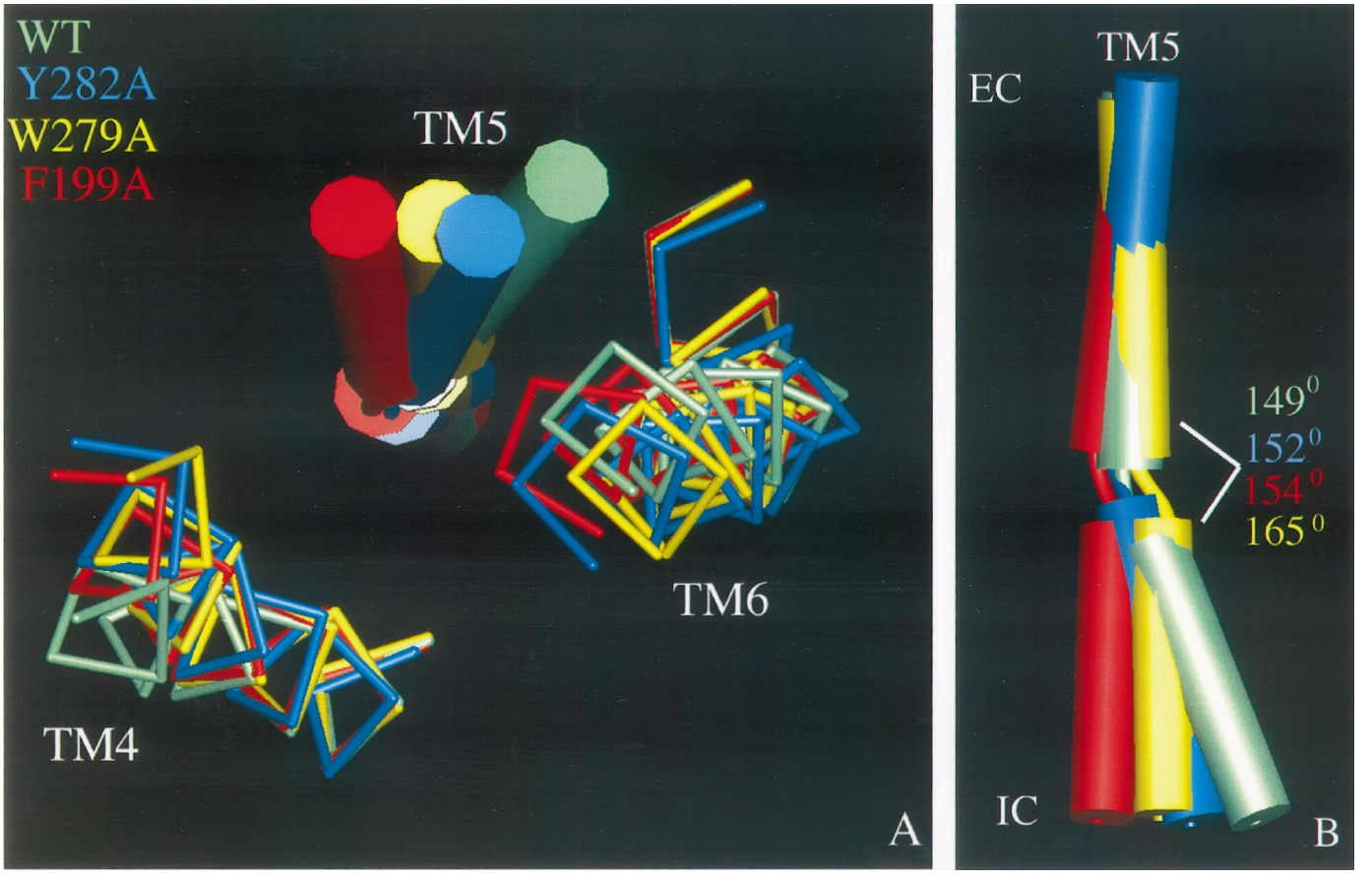

Fig. 9. A, Model of TM4, TM5, and TM6 of the WT, F199A, W279A, and Y282A TRH-Rs. The structures presented were extracted from averaged minimized structures derived from the last 200 psec of 1-nsec simulations. The receptor is positioned so that its extracellular domain is in the background and its intracellular domain in the foreground. B, TM5 from A positioned so that the extracellular domain (*EC*) of the receptor is at the *top*. *IC*, intracellular domain. The kink angles were calculated between two helical axes determined using the CHARMM program. The helical axes are defined by residues Pro190 through Pro203 and Pro203 through Phe213.

maximal signaling of only 37% of WT TRH-R levels (Perlman *et al*., 1997). Therefore, a number of conserved residues appear to be involved in intramolecular interactions that constrain receptors of the rhodopsin/β-adrenergic subfamily of GPCRs in an inactive state.

Our model predicts that there is increased motion in the intracellular portion of TM5 in the TRH-R, compared with the extracellular end. Pro203 in TM5, which is highly conserved in the rhodopsin/β-adrenergic receptor subfamily, appears to cause formation of a kink in the helix that could allow for the differences in motion at the two ends of the same helix. We have calculated the extent of the kink in TM5 in our model as the angle between two helical axes defined by the portions of the helix before and after the kink. This algorithm was implemented in the program CHARMM (Brooks *et al*., 1983). The axis before the kink is defined by the Cα atoms of residues 190–203 and the one after the kink by the Cα atoms of residues 203–213. The results obtained from the analysis performed over the last 500 psec of the trajectories show that in WT TRH-R the average kink angle is 153 ± 4°, whereas in the TRH-occupied receptor the value is 162 ± 7°. A similar analysis of the mutant receptors shows that in the Y200A TRH-R the kink angle is 146 ± 4°, whereas in the more constitutively active receptors Y282A TRH-R, F199A TRH-R, and W279A TRH-R the values are 154 ± 4°, 157 ± 3°, and 165 ± 3°, respectively. A statistical analysis (*t* test) shows that the values for the TRH-occupied F199A and W279A TRH-Rs are significantly different ($p < 0.05$) from those for WT and Y200A TRH-Rs. Fig. 9B presents the kink angles measured in the average structures that were energy-minimized over the last 200 psec of the trajectories; these findings suggest that, in the occupied and constitutively active receptors, TM5 has a tendency to straighten out and reduce the proline kink.

It has been suggested that, because the kink region does not have a periodicity of 3.6 amino acids/turn, a twisting of the faces occurs after the proline kink, relative to a straight helix (Ballesteros and Weinstein, 1992; Sankararamakrishnan and Vishveshwara, 1992). If the TM proline residues can be thought of as local helical hinge points allowing two separate rigid bodies to be functionally separated, as suggested by Woolf (1997), then twisting of the two separate domains around the proline residue is also likely to occur. In this work, we observed that, in the average structures, the intracellular part of TM5 appears to undergo a more significant rotation in the constitutively active F199A and W279A receptors than in the inactive Y200A and Y200F receptors, which leads us to suggest that straightening of the helical kink is associated with a significant twist of the intracellular portion of TM5.

Therefore, our results suggest that a release of the constraint imposed by Trp279 or Phe199 near the top of TM6 and TM5 results in increased distances between the intracellular portions of TM5 and TM6, as well as a conformational change transduced through TM5 to intracellular loop 3, which is known to be critical for activation of the TRH-R (Nussenzveig *et al*., 1993). These changes in the intracellular portion are accomplished by the unkinking of the proline kink in the middle of the helix and by a conformational change that can be represented as a face-twisting of the lower portion of TM5.

In conclusion, a model of the TRH-R was presented that predicts that Trp279 and Phe199 belong to the same hydrophobic cluster and are important for constraining the TRH-R in an inactive conformation. Experimental support for the model was obtained by showing that replacement of Phe199 and Trp279 by alanine results in constitutively active receptors with greater basal activity, compared with WT TRH-R. We propose that Trp279 in TM6 and at least Phe199 in TM5 hold the TRH-R in an inactive conformation by participating in interhelical interactions within a hydrophobic cluster of residues. Upon disruption of this hydrophobic pocket, either by TRH occupancy or by substitution of Trp279 or Phe199 with alanine, there is a release of these constraining interactions that leads to a change in the position and conformation of TM5. This change can be transmitted to intracellular loop 3, which has been shown to be important in TRH-R activation (Nussenzveig *et al*., 1993). We think that these changes are involved in TRH-R activation and may be part of a general mechanism of GPCR activation.

References

Altenbach C, Yang K, Farrens DL, Farahbakhsh ZT, Khorana HG, and Hubbell WL (1996) Structural features and light dependent changes in the cytoplasmic interhelical E-F loop region of rhodopsin: a site directed spin labeling study. *Biochemistry* **35:**12470–12478.

Arvanitakis L, Geras-Raaka E, and Gershengorn MC (1998) Constitutively signaling G protein-coupled receptors and human disease. *Trends Endocrinol Metab* **9:**27–31.

Baldwin JM (1994) Structure and function of receptors coupled to G proteins. *Curr Opin Cell Biol* **6:**180–190.

Ballesteros JA and Weinstein H (1992) Analysis and refinement of criteria for predicting structure and relative orientations of transmembranal helical domains. *Biophys J* **62:**107–109.

Brooks BR, Bruccoleri RE, Olafson BD, States DJ, Swaminathan S, and Karplus M (1983) CHARMM: a program for macromolecular energy minimization and dynamics calculations. *J Comp Chem* **4:**187–217.

Cohen DP, Thaw CN, Varma A, Gershengorn MC, and Nussenzveig DR (1997) Human calcitonin receptors exhibit agonist-independent (constitutive) signaling activity. *Endocrinology* **138:**1400–1405.

Colson AO, Perlman JH, Smolyar A, Gershengorn MC, and Osman R (1998) Static and dynamic roles of extracellular loops in G-protein-coupled receptors: a mechanism for sequential binding of thyrotropin-releasing hormone to its receptor. *Biophys J* **74:**1087–1100.

Farrens DL, Altenbach C, Yang K, Hubbell WL, and Khorana HG (1996) Requirement of rigid body motion of transmembrane helices for light activation of rhodopsin. *Science (Washington DC)* **274:**768–770.

Gershengorn MC and Osman R (1996) Molecular and cellular biology of thyrotropin-releasing hormone (TRH) receptors. *Physiol Rev* **76:**175–191.

Gether U, Ballesteros JA, Seifert R, Sanders-Bush E, Weinstein H, and Kobilka BK (1997) Structural instability of a constitutively active G protein-coupled receptor: agonist-independent activation due to conformational flexibility. *J Biol Chem* **272:**2587–2590.

Groblewski T, Maigret B, Larguier R, Lombard C, Bonnafous JC, and Marie J (1997) Mutation of Asn^{111} in the third transmembrane domain of the AT_{1A} angiotensin II receptor induces its constitutive activation. *J Biol Chem* **272:**1822–1826.

Javitch JA, Ballesteros JA, Weinstein H, and Chen JY (1998) A cluster of aromatic residues in the sixth membrane-spanning segment of the dopamine D2 receptor is accessible in the binding-site crevice. *Biochemistry* **37:**998–1006.

Jinsi-Parimoo A and Gershengorn MC (1997) Constitutive activity of native thyrotropin-releasing hormone receptors revealed using a protein kinase C-responsive reporter gene. *Endocrinology* **138:**1471–1475.

Kjelsberg MA, Cotecchia S, Ostrowski J, Caron MG, and Lefkowitz RJ (1992) Constitutive activation of the α_{1B}-adrenergic receptor by all amino acid substitutions at a single site: evidence for a region which constrains receptor activation. *J Biol Chem* **267:**1430–1433.

Konopka JB, Margarit SM, and Dube P (1996) Mutation of Pro-258 in transmembrane domain 6 constitutively activates the G protein-coupled α-factor receptor. *Proc Natl Acad Sci USA* **93:**6764–6769.

Laakkonen L, Guarnieri F, Perlman JH, Gershengorn MC, and Osman R (1996) A refined model of the thyrotropin-releasing hormone (TRH) binding pocket: novel mixed mode Monte Carlo/stochastic dynamics simulations of the complex between TRH and TRH receptor. *Biochemistry* **35:**7651–7663.

Lefkowitz RJ, Cotecchia S, Samama P, and Costa T (1993) Constitutive activity of receptors coupled to guanine nucleotide regulatory proteins. *Trends Pharmacol Sci* **14:**303–307.

Lin SW and Sakmar TP (1996) Specific tryptophan UV-absorbance changes are probes of the transition of rhodopsin to its active state. *Biochemistry* **35:**11149–11159.

Lin ZL, Shenker A, and Pearlstein R (1997) A model of the lutropin/choriogonadotropin receptor: insights into the structural and functional effects of constitutively activating mutations. *Protein Eng* **10:**501–510.

Matus-Leibovitch N, Nussenzveig DR, Gershengorn MC, and Oron Y (1995) Truncation of the thyrotropin-releasing hormone carboxyl tail causes constitutive ac-

tivity and leads to impaired responsiveness in *Xenopus* oocytes and AtT-20 cells. *J Biol Chem* **270:**1041–1047.
Nakayama TA and Khorana HG (1991) Mapping of the amino acids in membrane-embedded helices that interact with the retinal chromophore in bovine rhodopsin. *J Biol Chem* **266:**4269–4275.
Nussenzveig DR, Heinflink M, and Gershengorn MC (1993) Decreased levels of internalized thyrotropin-releasing hormone receptors after uncoupling from guanine nucleotide-binding protein and phospholipase-C. *Mol Endocrinol* **7:**1105–1111.
Nussenzveig DR, Thaw CN, and Gershengorn MC (1994) Inhibition of inositol phosphate second messenger formation by intracellular loop 1 of a human calcitonin receptor: expression and mutational analysis of synthetic receptor genes. *J Biol Chem* **269:**28123–28129.
Perlman JH, Colson A-O, Wang W, Bence K, Osman R, and Gershengorn MC (1997) Interactions between conserved residues in transmembrane helices 1, 2 and 7 of the thyrotropin-releasing hormone receptor. *J Biol Chem* **272:**11937–11942.
Perlman JH, Laakkonen LJ, Guarnieri F, Osman R, and Gershengorn MC (1996) A refined model of the thyrotropin-releasing hormone (TRH) receptor binding pocket: experimental analysis and energy minimization of the complex between TRH and TRH receptor. *Biochemistry* **35:**7643–7650.
Perlman JH, Laakkonen L, Osman R, and Gershengorn MC (1995) Distinct roles for arginines in transmembrane helices 6 and 7 of the thyrotropin-releasing hormone receptor. *Mol Pharmacol* **47:**480–484.
Probst WC, Snyder LA, Schuster DI, Brosius J, and Sealfon SC (1992) Sequence alignment of the G-protein coupled receptor superfamily. *DNA Cell Biol* **11:**1–20.
Quitterer U, AbdAlla S, Jarnagin K, and Muller-Esterl W (1996) Na^+ ions binding to the bradykinin B_2 receptor suppress agonist-independent receptor activation. *Biochemistry* **35:**13368–13377.
Robinson PR, Cohen GB, Zhukovsky EA, and Oprian DD (1992) Constitutively active mutants of rhodopsin. *Neuron* **9:**719–725.
Samama P, Cotecchia S, Costa T, and Lefkowitz RJ (1993) A mutation-induced activated state of the β_2-adrenergic receptor: extending the ternary complex model. *J Biol Chem* **268:**4625–4636.
Sankararamakrishnan R and Vishveshwara S (1992) Geometry of proline-containing *alpha*-helices in proteins. *Int J Peptide Protein Res* **39:**356–363.
Schadlow V, Barzilai N, and Deutsch PJ (1992) Regulation of gene expression in PC-12 cells via an activator of dual second messengers: pituitary adenylate cyclase-activating polypeptide. *Mol Biol Cell* **3:**941–951.
Scheer A, Fanelli F, Costa T, De Benedetti PG, and Cotecchia S (1996) Constitutively active mutants of the α_{1B}-adrenergic receptor: role of highly conserved polar amino acids in receptor activation. *EMBO (Eur Mol Biol Organ) J* **15:**3566–3578.
Spalding TA, Burstein ES, Brauner-Osborne H, Hill-Eubanks D, and Brann MR (1995) Pharmacology of a constitutively active muscarinic receptor generated by random mutagenesis. *J Pharmacol Exp Ther* **275:**1274–1279.
Tiberi M and Caron MG (1994) High agonist-independent activity is a distinguishing feature of the dopamine D1B receptor subtype. *J Biol Chem* **269:**27925–27931.
Van Rhee AM and Jacobson KA (1996) Molecular architecture of G protein-coupled receptors. *Drug Dev Res* **37:**1–38.
Wess J, Nanavati S, Vogel Z, and Maggio R (1993) Functional role of proline and tryptophan residues highly conserved among G protein-coupled receptors studied by mutational analysis of the m3 muscarinic receptor. *EMBO (Eur Mol Biol Organ) J* **12:**331–338.
Woolf TB (1997) Molecular dynamics of individual *alpha*-helices of bacteriorhodopsin in dimyristoyl phosphatidylcholine. I. Structure and dynamics. *Biophys J* **73:**2376–2392.
Yamano Y, Ohyama K, Kikyo M, Sano T, Nakagomi Y, Inoue Y, Nakamura N, Morishima I, Guo D-F, Hamakubo T, and Inagami T (1995) Mutagenesis and the molecular modeling of the rat angiotensin II receptor (AT_1). *J Biol Chem* **270:**14024–14030.

Send reprint requests to: Dr. Marvin C. Gershengorn, Cornell University Medical College, 1300 York Avenue, Room A328, New York, NY 10021. E-mail: mcgersh@mail.med.cornell.edu